Shape retaining self-healing metal-coordinated hydrogels

Alvaro Charlet[†], Viviane Lutz-Bueno[‡], Raffaele Mezzenga[‡#], and Esther Amstad[†]*

[†]Soft Materials Laboratory, Institute of Materials, EPFL Lausanne, Lausanne 1015, Switzerland

[‡]Laboratory of Food and Soft Materials Science, Department of Health Sciences and Technology, ETH Zurich, Zurich 8092, Switzerland

Department of Materials, ETH Zurich, Zurich 8093, Switzerland

Supplementary Movie S1. A 500 g brass weight is glued underwater to an inox flat surface using 2gPEG hydrogel glue crosslinked by Ca^{2+}.

Supplementary Movie S2. Hydrogels crosslinked with different ions are cut into two pieces and their self-healing behavior is monitored over time. From left to right, samples are composed of 2cPEG Fe^{3+}, 2gPEG Ca^{2+}, 2gPEG Zn^{2+} and 2gPEG Fe^{3+}. We assign the difference in the self-healing kinetics to the different relaxation times of the metal-coordination sites.

Supplementary Movie S3. The actuation of 2gPEG crosslinked by iron oxide nanoparticles with an external magnetic field.

Fitting of the SAXS data

Small-angle X-ray scattering is a powerful tool to explore the structure of materials at small-scales. The intensity I of elastically scattered X-rays is measured as a function of the scattering vector q.

Neutral semi dilute polymer solutions at equilibrium have their scattering intensity described by a Lorentzian function[1,2], in which the correlation length ξ varies with the volume fraction φ, according to $\xi_S \propto \varphi^{-3/4}$. This is only valid for $q < {}^{1}/_{\xi}$.

$$I(q) = \alpha\left(\rho_p - \rho_d\right)^2 \frac{kT\varphi}{\left(\frac{\partial \Pi}{\partial \varphi}\right)} \frac{1}{1 + Q^2 {\xi_S}^2}$$

$$\propto \alpha\left(\rho_p - \rho_d\right)^2 \sqrt{\frac{2}{\Pi}} \frac{\varphi^2 {\xi_S}^3}{1 + Q^2 {\xi_S}^2} \quad (1)$$

Where α is an instrumental constant, ρ_p and ρ_d are the scattering intensities of the polymer and solvent respectively.

In crosslinked networks, the polymer chains behave as transient networks with nonuniformities that depend on the distribution and concentration of ions/particles in the sample. The scattering intensity of the hydrogel cannot be described by Lorentzian functions for regions, because the restriction of movement imposed to the polymer chains by the crosslinks, must be included. This restricted movement has a Gaussian spatial distribution that can be modelled by the concentration correlation function.[1,3]

$$g_{1(r)} = \frac{\langle \delta\varphi^2 \rangle}{\langle \varphi \rangle} exp\left(-\frac{r^2}{2\psi^2}\right) \quad (2)$$

Where $\langle \delta\varphi^2 \rangle$ is the mean square amplitude of the concentration variations due to the effects of crosslinking, ψ is their mean size, and $\langle \varphi \rangle$ is the average concentration.
At the same time, the polymer chains can also have short-range fluctuations in between crosslinks, like in a polymer solution. The long-range (polymer chains at the junction points) and short-range fluctuations ("free" polymers between the crosslinks) are assumed to be decoupled.

The scattering curve is modelled by two terms: (i) a solution-like part with the shape of a Lorentzian, and (ii) a static part due to cross-links, which is the Fourier transform of a Gaussian. The total scattering function is then:

$$I(Q) = \alpha\left(\rho_p - \rho_d\right)^2 \left[\sqrt{\frac{2}{\Pi}}\, \frac{\varphi^2 {\xi_S}^3}{1+Q^2 {\xi_S}^2} + \langle \delta\varphi^2 \rangle\, \psi^3 exp\left(-\frac{Q^2\psi^2}{2}\right)\right] \quad (3)$$

1. Mallam, S., Horkay, F., Hecht, A. M., Rennie, A. R. & Geissler, E. Microscopic and macroscopic thermodynamic observations in swollen poly(dimethylsiloxane) networks. *Macromolecules* **24**, 543–548 (1991).
2. De Gennes, P.-G., 1932-2007 (viaf)68972558. *Scaling concepts in polymer physics*. (Ithaca (N.Y.) : Cornell university press, 1979).
3. Mallam, S., Hecht, A., Geissler, E. & Pruvost, P. Structure of swollen polydimethyl siloxane gels. *J. Chem. Phys.* **91**, 6447–6454 (1989).

The reversible gelation of 2gPEG hydrogels

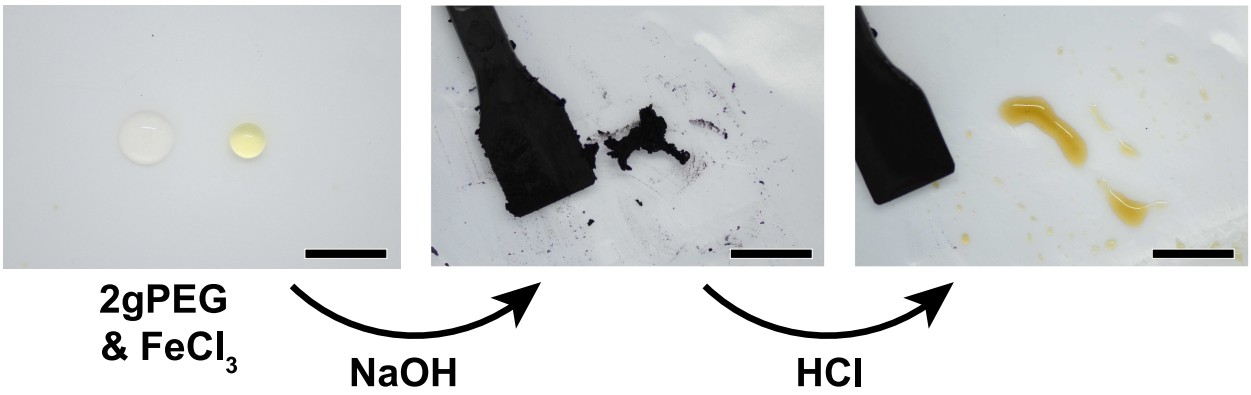

Figure S1. A 2gPEG solution containing Fe^{3+} ions is mixed with a NaOH solution (left). The hydrogel forms immediately upon manual mixing of the solutions (center). The addition of HCl immediately dissolves the hydrogel back to the liquid state. The change in color hints at the oxidation of some of the pyrogallols (right). The scale bar is 1 cm.

Oxidation of 2gPEG

Figure S2. Photograph of a 2gPEG solution exposed to NaOH in the absence of ions. After 24h, the solution appears yellow. The color change is a fingerprint for the oxidation of aromatic groups such as pyrogallols. The solution remains liquid, indicating that the oxidation of 2gPEG does not trigger gelation. The scale bar is 5 mm.

XRD spectroscopy

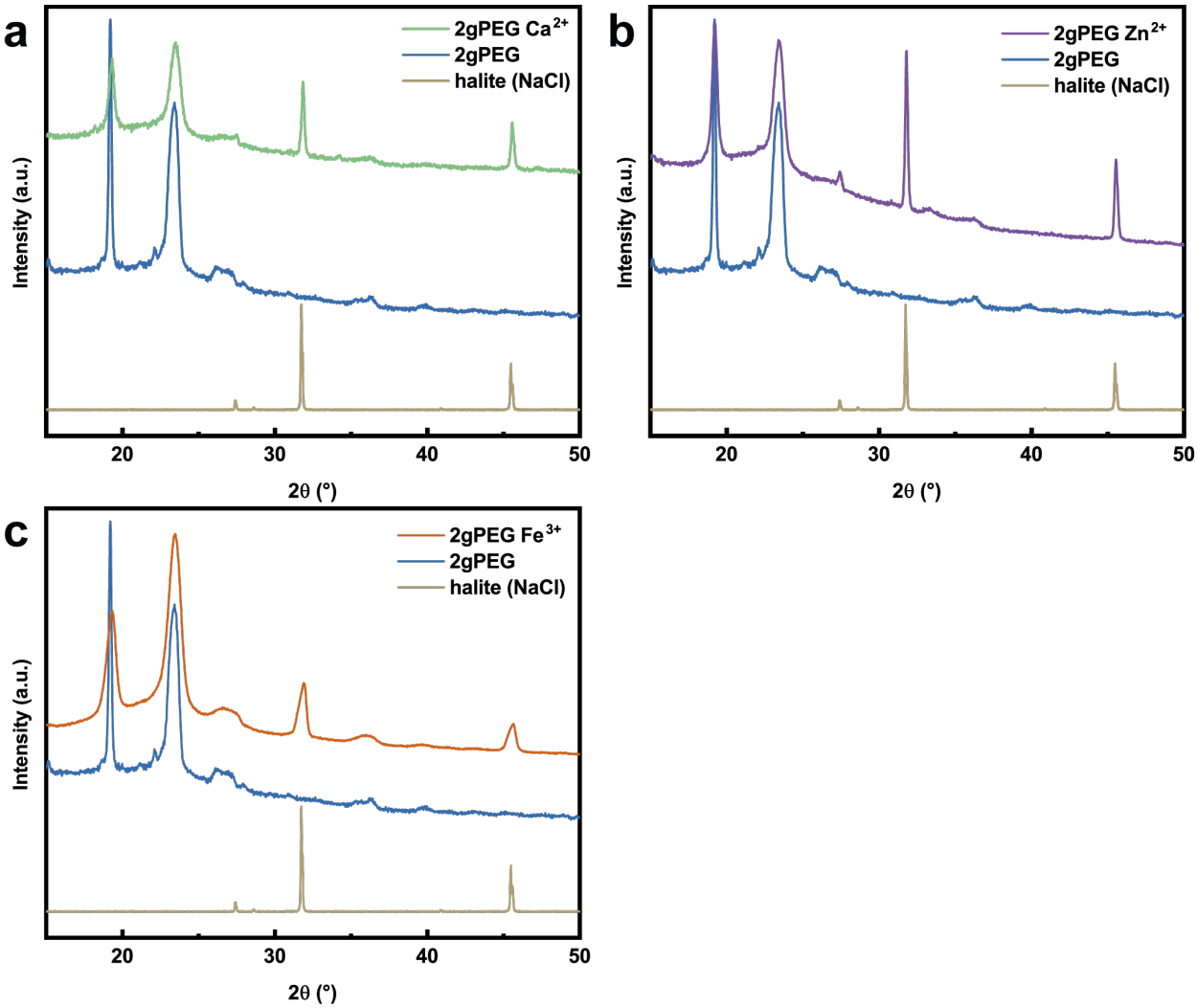

Figure S3. XRD diffraction spectra of dried 2gPEG hydrogels that have been crosslinked with (a) Ca^{2+}, (b) Zn^{2+}, and (c) Fe^{3+} are compared to the bare dry 2gPEG and the diffraction pattern of NaCl (RRUFF database). A comparison between the spectra reveals that the observed diffraction peaks are due to the crystalline domains of PEG and NaCl crystals. No other diffractions can be identified.

SAXS analysis

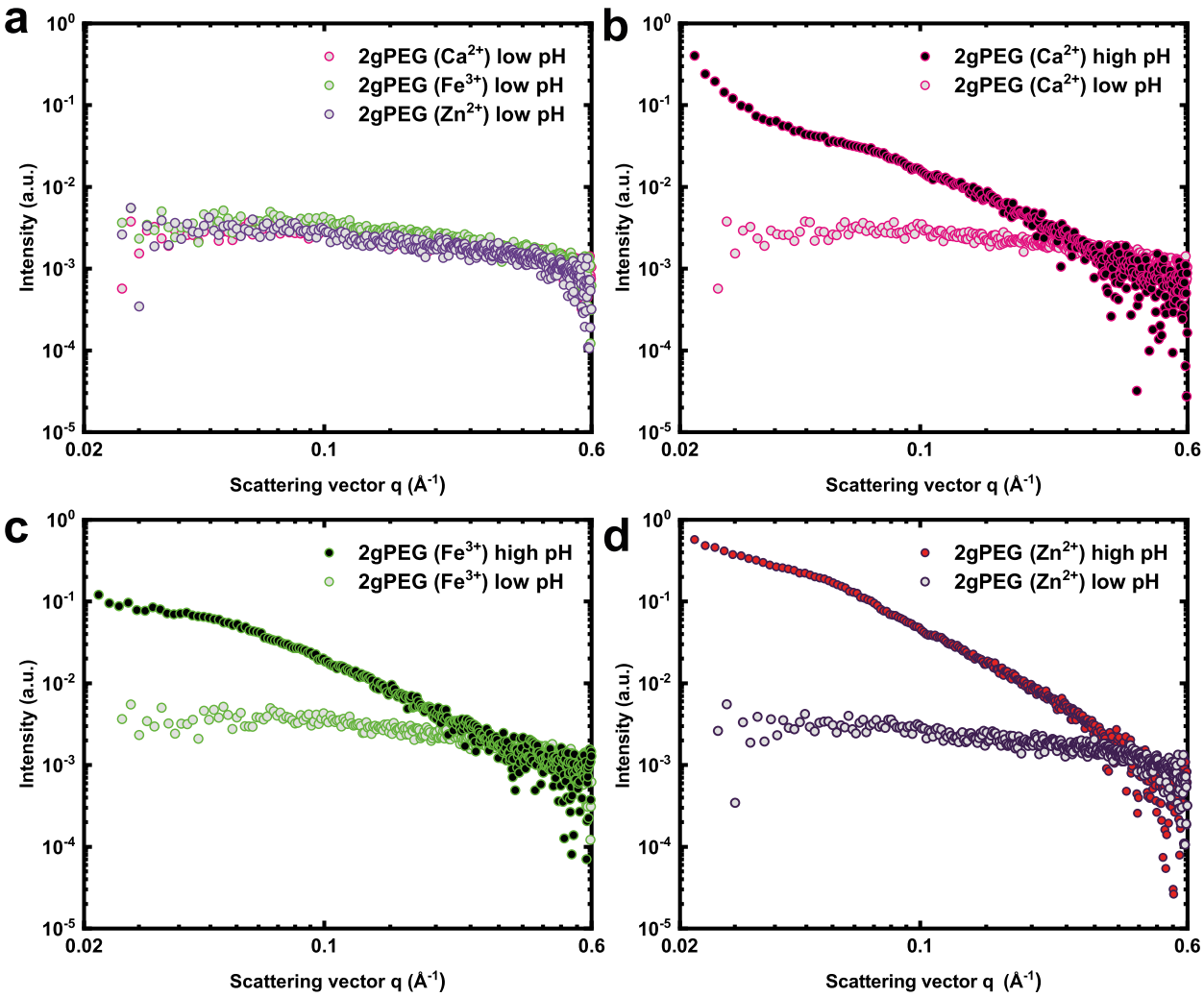

Figure S4. (a) Scattering of the 2gPEG solutions containing Ca^{2+}, Fe^{3+} and Zn^{2+} ions at low pH. (b-d) Scattering of the low pH solutions of 2gPEG containing (b) Ca^{2+}, (c) Fe^{3+}, and (d) Zn^{2+} respectively (light grey fill); and of the high pH Ca^{2+}, Fe^{3+}, and Zn^{2+} hydrogels (black fill).

Particle precipitation in the absence of pyrogallol groups

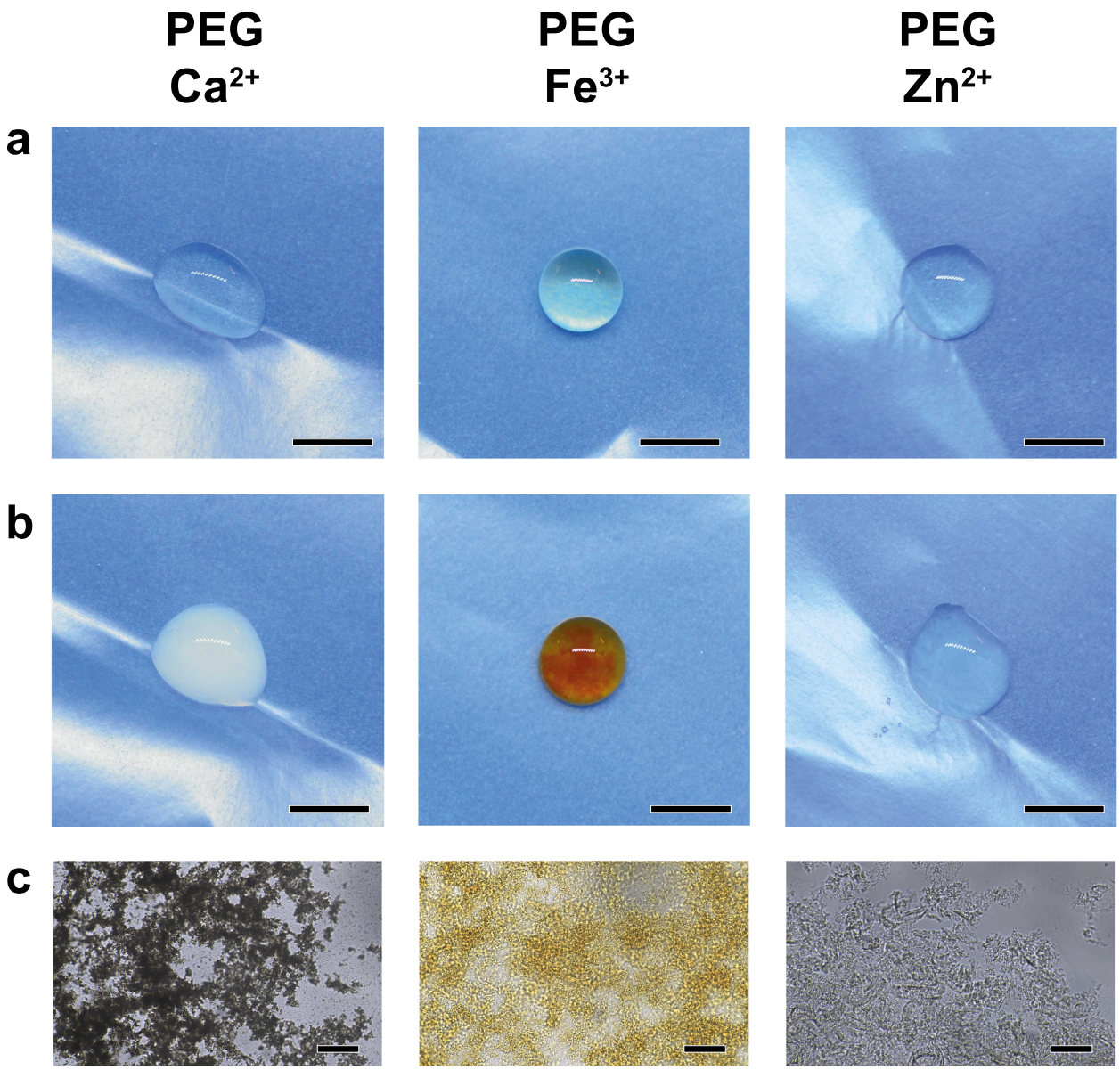

Figure S5. Photographs of PEG solutions, containing Ca^{2+}, Fe^{3+}, and Zn^{2+} ions. (a) The concentrations of PEG and the ions are the same as in the solutions used to prepare 2gPEG hydrogels (scale bar is 5 mm). (b) The pH shift induced through the addition of NaOH triggers the precipitation of microparticles, visible to the naked eye (scale bar in 5 mm). (c) Micrographs of the microparticles in suspension (scale bar is 200 µm).

Raman spectroscopy of 2gPEG hydrogels

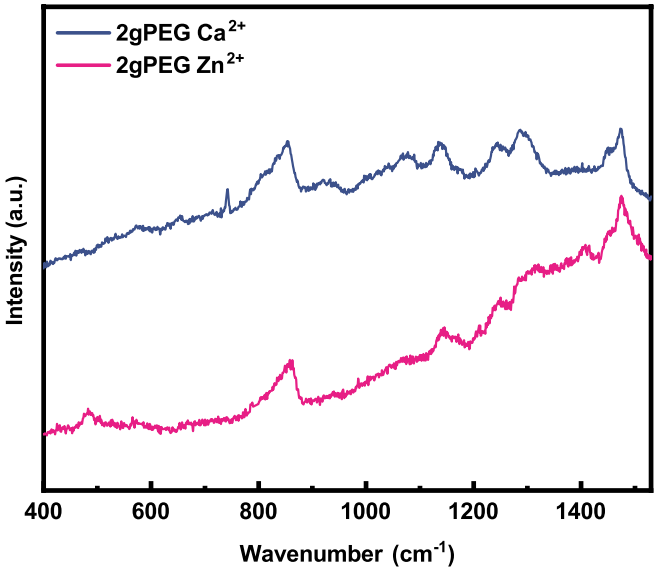

Figure S6. Raman shift spectrum of 2gPEG crosslinked with Ca^{2+} and Zn^{2+}. No peaks are observed in the range of 500-680 cm^{-1}.

Vibrational spectroscopy of as-synthesised 2gPEG

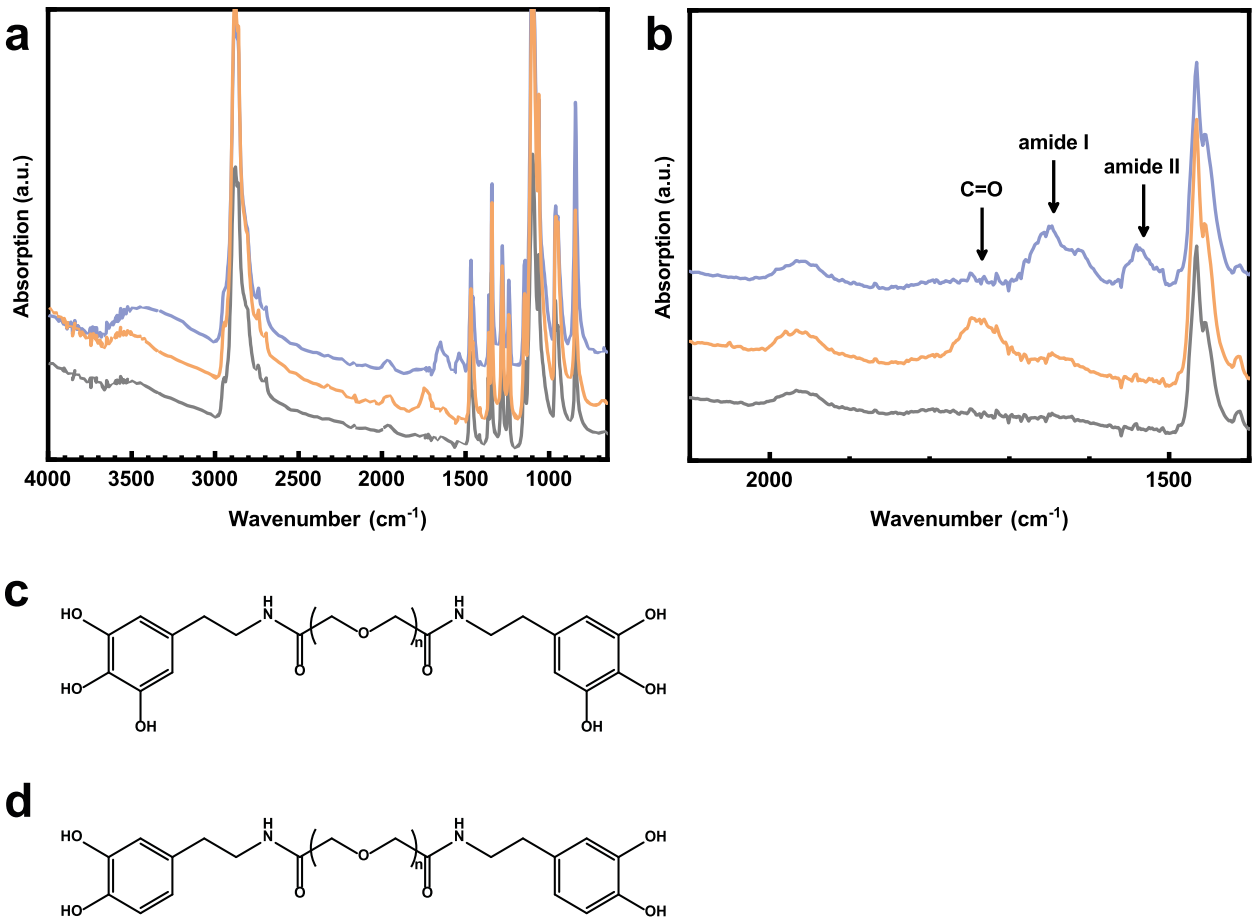

Figure S7. (a-b) FTIR spectra of 2gPEG (top, blue), PEG-di-COOH (middle, orange), and PEG (bottom, grey). The carboxylic end-group functionalization of PEG is validated by the C=O stretch at 1760 cm^{-1}. The further coupling of the carboxylic group with the amine of 5-hydroxydopamine is validated by the presence of the amide I and II stretches at 1650 and 1550 cm^{-1} respectively. (c) Chemical structure of the 2gPEG molecule. (d) Chemical structure of the 2cPEG molecule.

NMR spectroscopy of as-synthesised 2gPEG

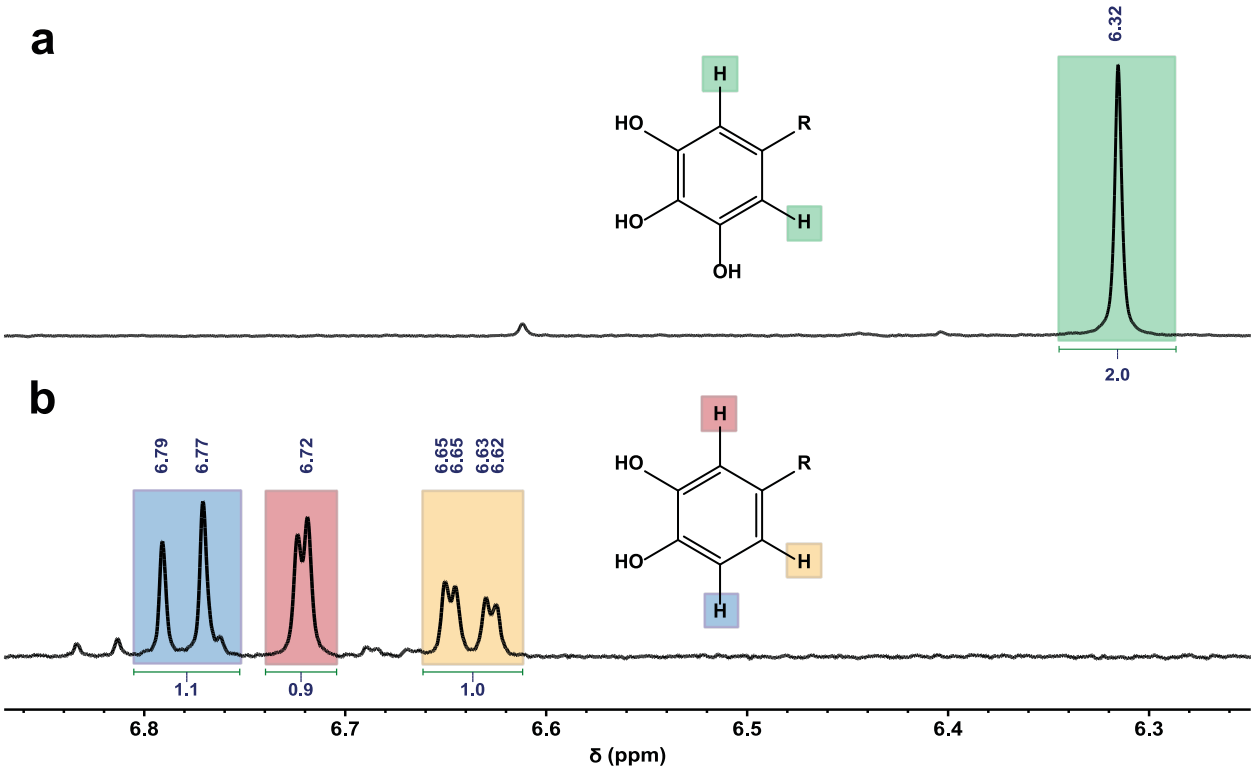

Figure S8. ^{1}H NMR spectra of 2gPEG (top) and 2cPEG (bottom) in D_2O. Spectrum of 2gPEG: 1H NMR (400 MHz, Deuterium Oxide) δ 6.32 (s, 2H). Spectrum of 2cPEG: 1H NMR (400 MHz, Deuterium Oxide) δ 6.78 (d, J = 8.1 Hz, 1H), 6.72 (s, 1H), 6.64 (dd, J = 8.1, 2.1 Hz, 1H).

Raman spectrosocpy of as-synthesised dry 2gPEG

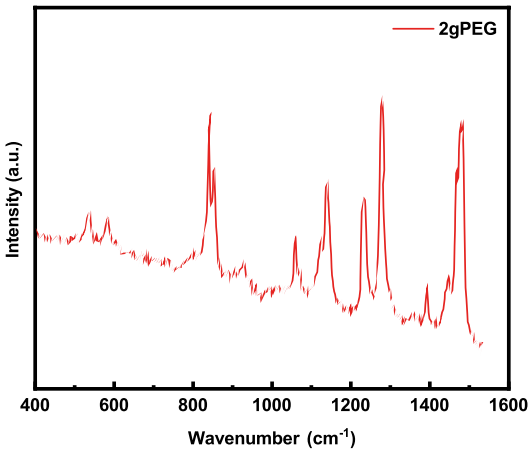

Figure S9. Raman shift spectrum of 2gPEG in the dry state.